

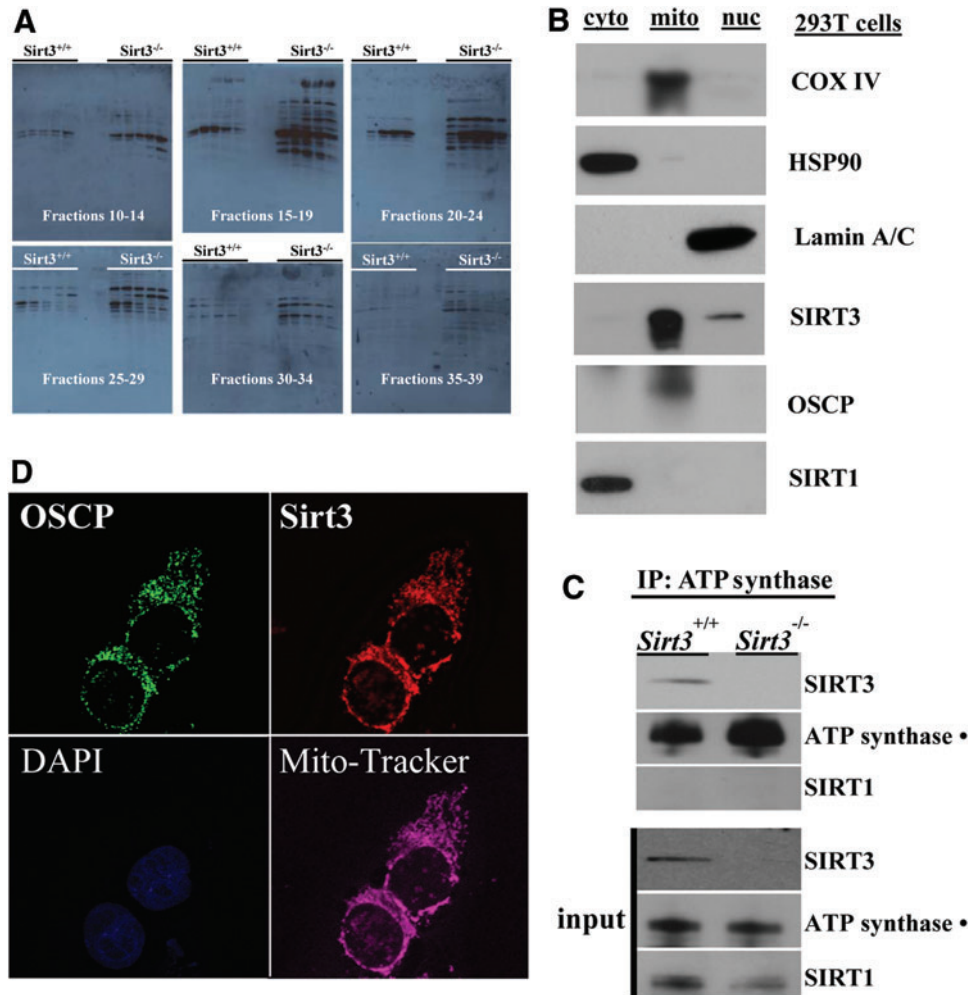
Supplementary Data

Supplementary Methods

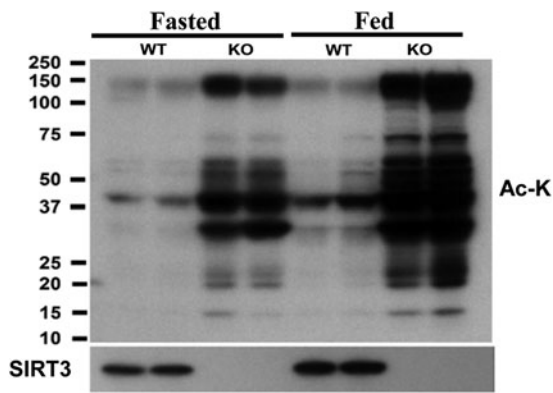
Mass spectrometry sample preparation

Percutaneous muscle biopsies of the *vastus lateralis* muscle from a bariatric surgery subject preoperative and 6 months postoperative were obtained under local anesthesia by conchotome with IRB approval. Muscle biopsy specimens

(50–75 mg) were immediately rinsed in ice-cold saline, blotted dry, then frozen, and stored in nitrogen until use. The muscle biopsies were homogenized while still frozen in an ice-cold buffer (10 μ l/mg tissue) consisting of (final concentrations) 20 mM HEPES, pH 7.6; 1 mM EDTA; 250 mM sucrose, 2 mM Na_3VO_4 ; 10 mM NaF; 1 mM sodium pyrophosphate; 1 mM ammonium molybdate; 250 μ M PMSF;



SUPPLEMENTARY FIG. S1. Liver mitochondria from $Sirt3^{-/-}$ mice exhibit increased lysine acetylation. (A) Mitochondrial proteins from isogenic, matched 3-month-old $Sirt3^{-/-}$ mouse liver demonstrate increased acetylation. Liver mitochondria from $Sirt3$ wild-type ($Sirt3^{+/+}$) and knockout ($Sirt3^{-/-}$) mice were purified and solubilized. The solubilized protein was separated by ion-exchange chromatography and six selected fractions (10–14, 15–19, 20–24, 25–29, 30–34, and 35–39) were further resolved by sodium dodecyl sulfate polyacrylamide gel electrophoresis (SDS-PAGE), transferred to polyvinylidene difluoride (PVDF) membranes, and probed with an antibody against acetyl-lysine (Cell Signaling, Inc.). These fractionated results clearly show the degree of differences in mitochondrial acetylation between the $Sirt3$ wild-type and knockout mouse livers. (B) 293T cells were subjected to subcellular fractionation. Cytosolic (cyto), mitochondrial (mito), and nuclear (nuc) fractions were subjected to SDS-PAGE, followed by immunoblotting with anti-SIRT3, oligomycin sensitivity-conferring protein (OSCP), and SIRT1. Antibodies against HSP90, COX IV, and Lamin A/C were used as controls for purity of cytoplasmic, mitochondrial, and nuclear fractions, respectively. (C) Skeletal muscle lysates from $Sirt3^{+/+}$ and $Sirt3^{-/-}$ mice were harvested, IPed with an anti-ATP synthase antibody (Abcam, Inc.), and subsequently immunoblotted with an anti-ATP synthase β subunit (Abcam, Inc.), anti-SIRT3 antibody (Cell Signaling, Inc.), and anti-SIRT1 antibody (Millipore, Inc.). (D) $Sirt3$ interacts with OSCP. Immunohistochemistry (IHC) staining with an OSCP antibody, DAPI, and mitotracker. Representative micrographs are shown.



SUPPLEMENTARY FIG. S2. *Sirt3* knockout cells have increased mitochondrial acetylated protein. Mitochondrial proteins from isogenic, matched three-month-old *Sirt3*^{-/-} mouse liver demonstrate increased acetylation. Liver mitochondria from *Sirt3* wild-type (*Sirt3*^{+/+}) and knockout (*Sirt3*^{-/-}) mice either fed or fasted were purified and immunoblotted with an anti-acetyl lysine (AcK) antibody (Cell Signaling).

10 μ g/ml leupeptin; 10 μ g/ml aprotinin; 5 μ M trichostatin A; and 10 mM nicotinamide. After being homogenized by a polytron homogenizer at maximum speed for 30 s, the homogenate was cooled on ice for 20 min and then centrifuged at 10,000 g for 20 min at 4°C; the resulting supernatant containing 2 mg of lysate supernatant proteins was used for in-solution digestion. Two milligrams of soluble protein (concentration determined by the Bio-Rad DC Protein Assay) was used for acetylated peptide enrichments. To prepare tryptic peptides for enrichment, aliquots of soluble protein from each sample homogenate were diluted for approximately 100 μ l with 1 M TrisHCl, pH 8.0 before the addition of 100 μ l trifluoroethanol (TFE). The samples were then reduced by the addition of 2 μ l of 0.5 M TCEP for 1 h at room temperature, and alkylated with 4 μ l of 500 mM iodoacetamide for 30 min in the dark at room temperature. Samples were diluted 10-fold with 100 mM Tris HCl, pH 8.0 to reduce the solution to 5% TFE, and digested overnight at 37°C with proteomic-grade trypsin (Sigma Chemical Co.) at a ratio of 1:40 enzyme to protein. The resulting peptides were then desalted by solid-phase extraction (Sep-pak C18 cartridges, Waters Corporation). Digested samples were first acidified with TFA, diluted two-fold with 0.1% TFA, and loaded *via* a syringe onto the Sep-pak SPE material. After sample loading, the cartridges were washed with 0.1% TFA and eluted *via* a step-wise elution with 10% to 80% acetonitrile/0.1% TFA. A 500 μ l elution volume was used for each acetonitrile elution step. Eluates were reduced to dryness *via* vacuum centrifugation.

Mass spectrometry-based proteomics. Liquid chromatography-tandem mass spectrometry (LC-MS-MS) analysis of the peptides was performed using a LTQ-Orbitrap mass spectrometer (Thermo Scientific) that was equipped with a nanospray source and an Eksigent NanoLC 1D Plus and AS1 Autosampler. The peptides were loaded onto a self-packed biphasic C18/SCX MudPIT column using a Helium-pressurized cell (pressure bomb). The MudPIT column consisted of 360 \times 150 μ m i.d. fused silica, fritted with a filter-end fitting (IDEX Health & Science), and packed with

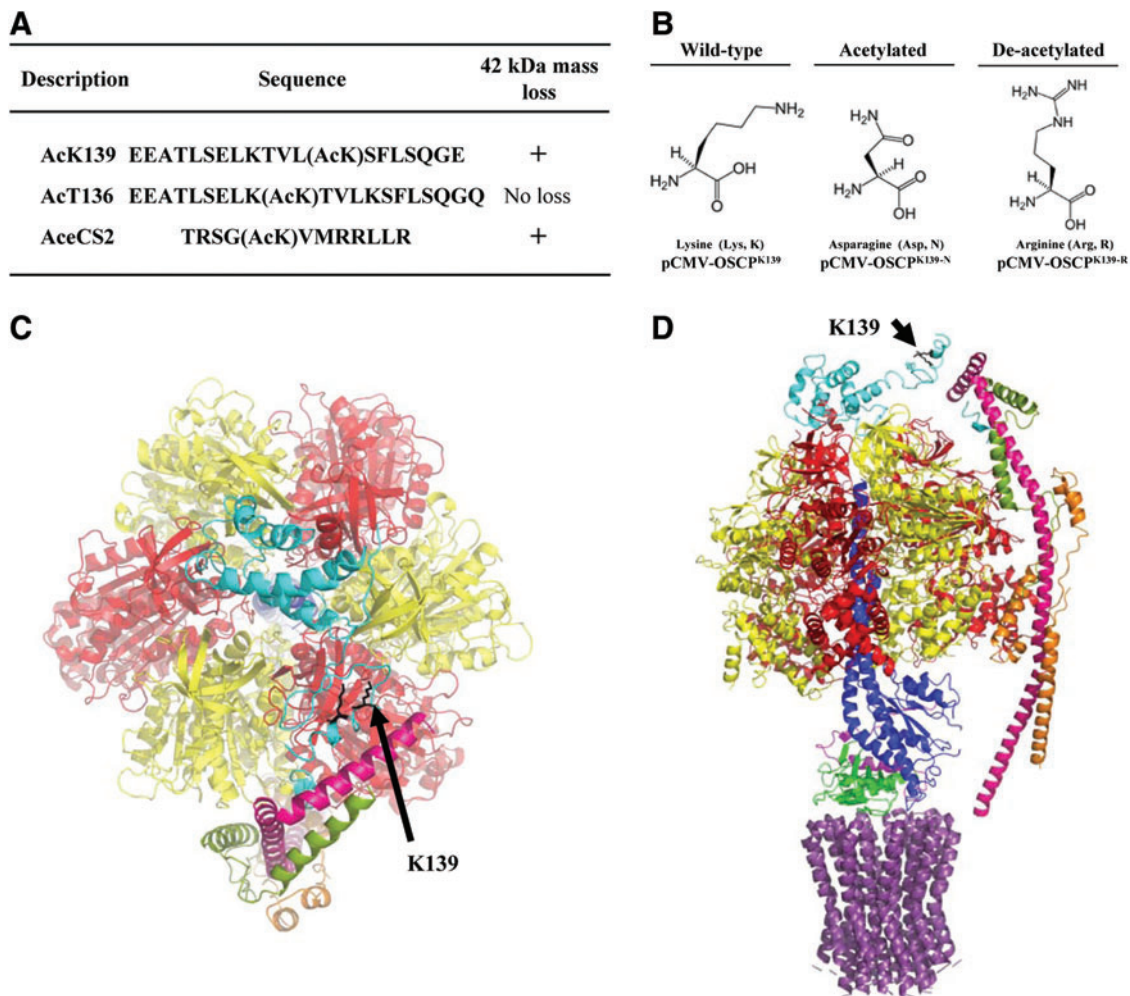
6 cm of Luna SCX material (5 μ m bead; Phenomenex) and 4 cm of Jupiter C18 material (5 μ m bead; Phenomenex). After sample loading, the MudPIT column was connected using an M-520 microfilter union (IDEX Health & Science) to an analytical column (360 \times 100 μ m i.d.), equipped with a laser-pulled emitter tip. The analytical column was packed with 20 cm Jupiter C18 material (3 μ m bead; Phenomenex). Using the Eksigent nanoLC and autosampler, MudPIT analysis was performed with a four-step salt pulse gradient (0 mM, 100 mM, 500 mM, and 1 M ammonium acetate). Peptides were eluted from the analytical column after each salt pulse with a 105 min reverse gradient (2%–45% Acetonitrile, 0.1% formic) for the first three salt pulses, and a 2%–95% Acetonitrile for the last salt pulse. Gradient-eluted peptides were introduced into the mass spectrometry *via* nanoelectrospray ionization.

Data were collected using a six-scan event, data-dependent method. Full scans (m/z 400–2000) were acquired with the Orbitrap as the mass analyzer (resolution 60,000), and the five most abundant ions in each MS scan were selected for fragmentation *via* collision-induced dissociation (CID) in the LTQ. An isolation width of 2 m/z , an activation time of 30 ms, 35% normalized collision energy, a maximum injection time of 150 ms, and an AGC target of 1×10^4 were used to generate MS/MS spectra. Dynamic exclusion was enabled, using a repeat count of two, a repeat duration of 5 s, and an exclusion duration of 15 s.

For the identification of acetylated peptides, raw data were extracted using ScanSifter (v2.1.25) and searched with SEQUEST (Thermo Fisher Scientific) against a human subset database created from the Uniprot KB protein database (www.uniprot.org). The protein database was a concatenated forward and reversed (decoy) database. Searches were configured to use variable modifications of +57.02146 on Cys (carbamidomethylation), +15.9949 on Met (oxidation), and +42.01056 on Lys (acetylation). Search results were assembled using Scaffold 3 (Proteome Software).

Co-immunoprecipitation

HCT116 cells stably expressing an Myc-tagged (EQKLI-SEEDL) WT *Sirt3*, or Myc-tagged null *Sirt3*, as well as cells possessing an empty vector, were cultured in five 100 mm dishes to a confluence of ~80%. The cells were washed twice with cold PBS and harvested on ice in the presence of a 1 ml/100 mm dish of lysis buffer (50 mM Tris, pH 7.4, 150 mM NaCl, 0.5 mM EDTA, 0.1% NP-40, and protease inhibitor cocktail 1 \times). Cells were scraped and lysed through one freeze thaw. Lysates were centrifuged at 14,000 rpm for 10 min, and the supernatant was incubated with 50 μ l Protein G Sepharose 4 Fast Flow (GE Healthcare) and 2 μ g of an antibody that was specific for either the Myc-tag (Cell Signaling, #2276) or oligomycin sensitivity-conferring protein (OSCP) (MitoSciences, #MS505) for 2 h at 4°C. The resin was washed thrice with wash buffer (50 mM Tris, pH 7.4, and 150 mM NaCl) and centrifuged at 4000 rpm for 30 s. After the final wash, the samples were incubated at 95°C for 5 min in 2 \times LDS (Invitrogen) containing a reducing agent. Protein samples were divided and resolved on 4%–12% Bis-Tris gels (Invitrogen) and transferred to nitrocellulose membranes (Protran). Membranes were probed with either a 1:2000 dilution of anti-OSCP or a 1:1000 dilution of anti-SIRT3 (Cell



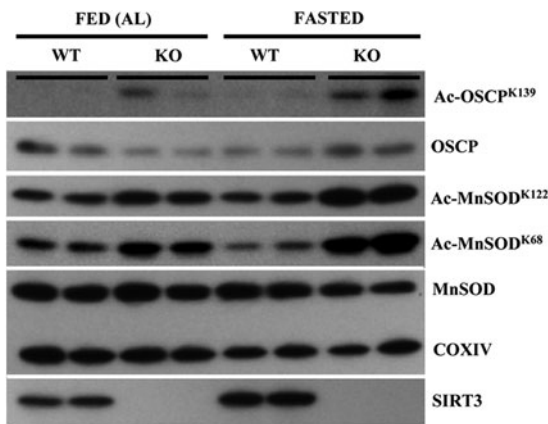
SUPPLEMENTARY FIG. S3. Acetylated lysine 139: position and variants. (A) Peptides from the sequence of OSCP were synthesized with either acetylated lysine 139 or threonine 136. A peptide derived from Acetyl CoA synthetase 2 (AceCS2) served as a positive control. *In vitro* deacetylation reactions were performed for all synthetic peptides and changes in *m/z* value, measured by MALDI-TOF, reflect changes in the acetylation state. (B) Schematic for the substitution of a lysine with asparagine (N) to mimic an acetylated amino acid state and with arginine (R) to mimic a deacetylated amino acid state (15, 22). (C, D) A representative side top view (C) and co-axial view (D) of a three-dimensional rendering of the protein structure for OSCP as a part of the complete ATP synthase (20). Lysine 139 is identified by a *black arrow*. As can be seen, lysine 139 is on the outside of the protein and, as such, is in an ideal position to interact with other proteins such as the SIRT3 deacetylase.

Signaling, #2627) and with secondary antibodies that were conjugated to horseradish peroxidase (Thermo). Blots were analyzed utilizing an ECL substrate (Pierce), Kodak X-OMAT Blue film (13 × 18 cm), and a Kodak film processor.

Sample preparation/acetylated peptide enrichment/mass spectrometry. Cells or tissues were lysed in lysis buffer without protease inhibitors, and the resulting supernatant containing 10 mg of protein was immediately used for TFE-assisted in-solution digestion. Aliquots of the protein lysate were diluted for approximately 100 μ l with 1 M TrisHCl, pH 8.0 before the addition of 100 μ l TFE. The samples were then reduced by the addition of 2 μ l of 0.5 M TCEP for 1 h at room temperature, and alkylated with 4 μ l of 500 mM iodoacetamide for 30 min in the dark at room temperature. Aliquots were then diluted 10-fold with 100 mM Tris HCl, pH 8.0 to reduce the solution to 5% TFE, and digested overnight at

37°C with proteomic-grade trypsin (Sigma Chemical Co.) at a ratio of 1:40 enzyme to protein. The resulting peptides were then desalted by solid-phase extraction (Sep-pak C18 cartridges, Waters Corporation). Digested samples were first acidified with TFA, diluted two-fold with 0.1% TFA, and loaded *via* a syringe onto the Sep-pak SPE material. After sample loading, the cartridges were washed with 0.1% TFA, and eluted *via* step-wise elution with 10% to 80% acetonitrile/0.1% TFA. A 1 ml elution volume was used for each acetonitrile elution step. Eluates were reduced to dryness *via* vacuum centrifugation.

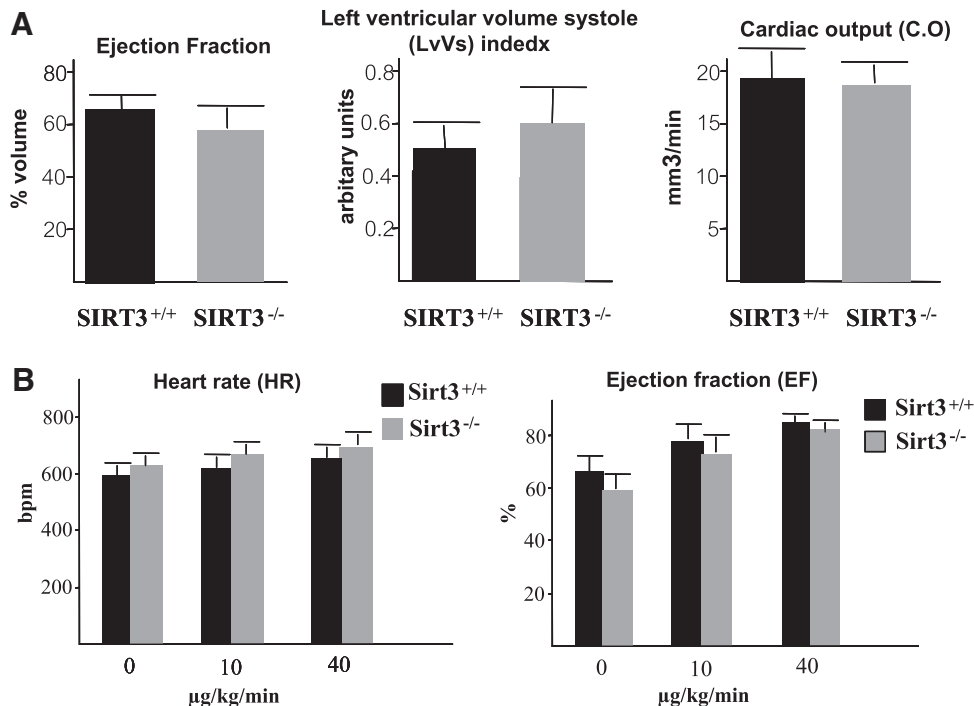
After solubilization of the dried peptides, acetylated peptides were enriched by using Protein-A conjugated agarose beads that were immobilized with anti-acetyllysine antibodies (ICP0388; ImmunoChem Pharmaceuticals, Inc.) in a 1 ml final volume of NETN buffer (50 mM Tris-HCl [pH 8.0], 100 mM NaCl, 1 mM EDTA, and 0.5% NP40), and the



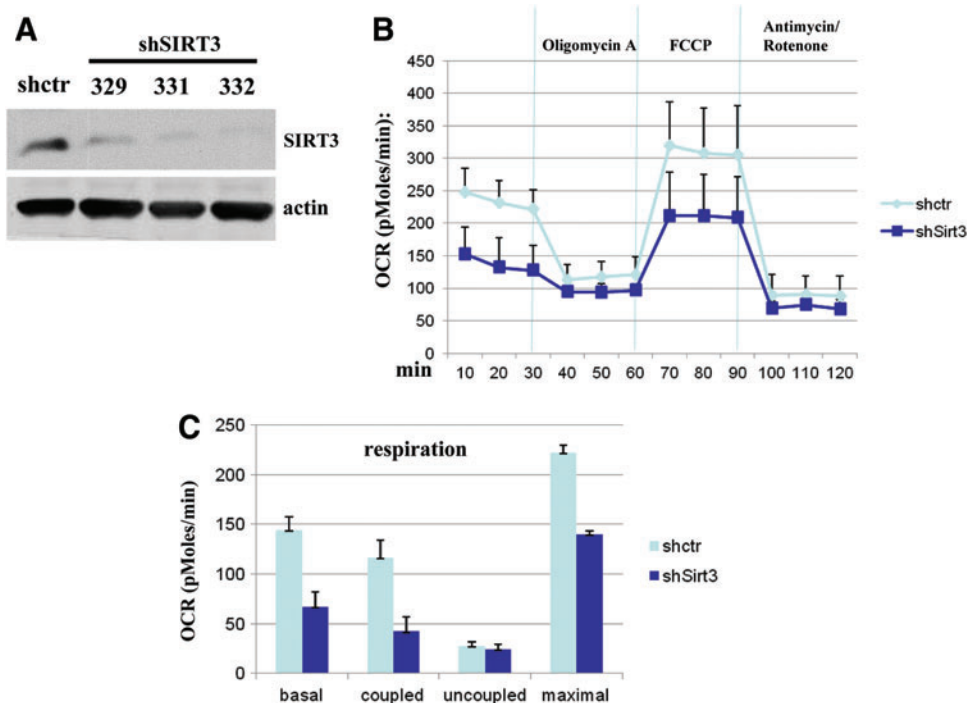
SUPPLEMENTARY FIG. S4. OSCP has a physiologically relevant reversible acetyl-lysine under nutrient stress. Livers from isogenic, three-month-old age-matched *Sirt3*^{+/+} mice fed or fasted for 36h were harvested and mitochondrial extracts were subsequently blotted with antibodies to MnSOD, Ac-MnSOD^{K122}, Ac-MnSOD^{K68}, OSCP, Ac-OSCP^{K139}, SIRT3, and COXIV.

mixture was incubated with rotation at 4°C for 4 h. The beads were washed thrice with 1 ml of NETN buffer and thrice with ETN (50 mM Tris-HCl [pH 8.0], 100 mM NaCl, and 1 mM EDTA). The bound peptides were eluted from the beads by washing thrice with 50 μ l of 0.1% TFA. The eluates were combined and dried by speedvac centrifugation. The peptides were reconstituted in 0.1% formic acid.

LC-MS-MS analysis of the peptides was performed using an LTQ Orbitrap Velos mass spectrometer (Thermo Scientific) that was equipped with a nanospray source and an Eksigent NanoLC Ultra and AS2 Autosampler. The peptides were loaded onto a self-packed biphasic C18/SCX MudPIT column using a Helium-pressurized cell (pressure bomb). The MudPIT column consisted of 360 \times 150 μ m i.d. fused silica, fritted with a filter-end fitting (IDEX Health & Science), and packed with 6 cm of Luna SCX material (5 μ m bead; Phenomenex) and 4 cm of Jupiter C18 material (5 μ m bead; Phenomenex). After sample loading, the MudPIT column was connected using an M-520 microfilter union (IDEX Health & Science) to an analytical column (360 \times 100 μ m i.d.), equipped with a laser-pulled emitter tip. The analytical column was packed with 20 cm Jupiter C18 material (3 μ m bead; Phenomenex). Using the Eksigent nanoLC and autosampler, MudPIT analysis was performed with an eight-step salt pulse gradient (0 mM, 100 mM, 150 mM, 200 mM, 300 mM, 500 mM, 750 mM, and 1 M ammonium acetate). Peptides were eluted from the analytical column after each salt pulse with a 105 min reverse gradient (2%–45% Acetonitrile, 0.1% formic) for the first three salt pulses, and a 2%–95% Acetonitrile for the last salt pulse. Gradient-eluted peptides were introduced into the mass spectrometry *via* nanoelectrospray ionization. Data were collected using a 17-scan event, data-dependent method. Full scans (*m/z* 350–2000) were acquired with the Orbitrap as the mass analyzer (resolution 60,000), and the five most abundant ions in each MS scan were selected for fragmentation *via* CID in the LTQ. An isolation width of 2 *m/z*, an activation time of 10 ms, 35% normalized



SUPPLEMENTARY FIG. S5. No difference in cardiac function between *Sirt3*^{+/+} and *Sirt3*^{-/-} mice under both basal and stressful conditions. (A) Cardiac magnetic resonance imaging (MRI) was performed in both wild-type *Sirt3* (+/+) and *Sirt3* knockout (-/-) 6-month-old mice. Ejection fraction (*left panel*), left ventricular volume systole (LvVs) (*middle panel*), and cardiac output (C.O) (*right panel*) were determined. (B) Changes in heart rate (HR) (*left*) and ejection fraction (EF) (*right*) during low (10 μ g/kg) and high (40 μ g/kg) dose dobutamine stress in both *Sirt3*^{+/+} and *Sirt3*^{-/-} mice. Experiments were done in triplicate, and error bars represent one standard deviation.



SUPPLEMENTARY FIG. S6. Sirt3 knockdown cells display decreased mitochondrial respiration. (A) Lysates from shctr C2C12 cells or C2C12 infected with three different shRNAs to knockdown Sirt3 were immunoblotted with anti-SIRT3 antibody. Actin was used as a loading control. (B, C) The respiratory profile of differentiated shctr C2C12 myotubes and shSirt3 knockdown C2C12 myotubes was assessed using a Seahorse Flux Analyzer. Blockers of different complexes in the mitochondrial electron transport chain were used, and changes in oxygen consumption rates were recorded before and after each drug injection. Basal mitochondrial respiration was calculated by subtraction of nonmitochondrial respiration (after antimycin/rotenone injection) from total basal respiration (before Oligomycin A injection). Coupled respiration was calculated by subtraction of respiration after Oligomycin A injection from total basal respiration. Uncoupled respiration was estimated by subtraction of nonmitochondrial respiration (after antimycin/rotenone injection) from coupled respiration (after Oligomycin A injection). Maximal respiration was assessed by subtraction of nonmitochondrial respiration (after antimycin/rotenone injection) from respiration after addition of the mitochondrial uncoupler Carbonyl cyanide 4-(trifluoromethoxy)-phenylhydrazone (FCCP).

collision energy, a maximum injection time of 100 ms, and an AGC target of 1×10^4 were used to generate MS/MS spectra. Dynamic exclusion was enabled, using a repeat count of 1, a repeat duration of 10 s, and an exclusion duration of 15 s.

For the identification of acetylated peptides, raw data were extracted using ScanSifter (v2.125) and searched with SEQUEST (Thermo Fisher Scientific) against a mouse subset database created from the Uniprot KB protein database (www.uniprot.org). The protein database was concatenated forward and reversed (decoy) database. Searches were configured to use variable modifications of +57.0214 on Cys (carbamidomethylation), +15.9949 on Met (oxidation), and +42.010565 on Lys (acetylation). Search results were assembled using Scaffold 3.3 (Proteome Software), and all tandem mass spectra of acetylated peptides were examined by manual interrogation using Xcalibur 2.1 Qual Browser software to validate sites of lysine acetylation.

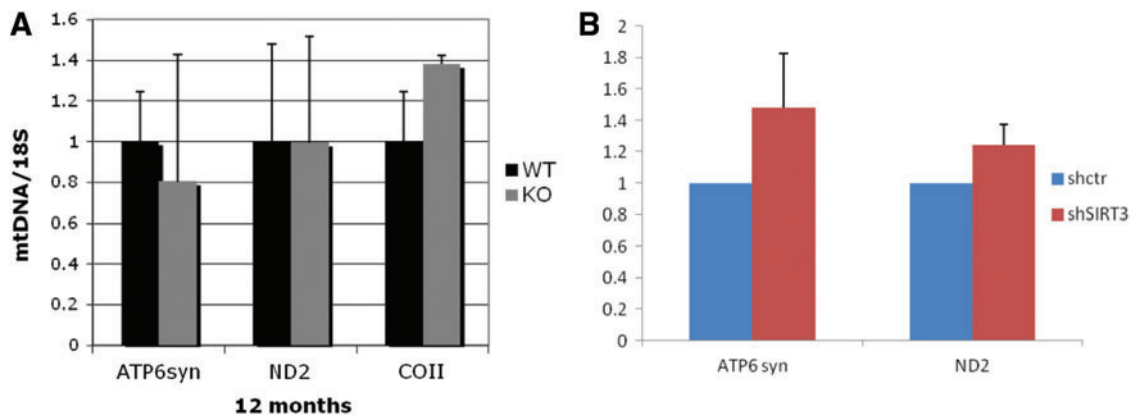
Calorie restriction and dietary considerations

Calorie restriction (CR) and 36 h of fasting were performed on wild-type and *Sirt3*-deficient mice using the NIA/NIH CR protocol (2) and our previous protocol (27), respectively. The mice are started on a CR diet beginning at 3 months with a stepwise reduction in caloric intake beginning with 10%

restriction at 14 weeks, increasing to 25% restriction at 15 weeks, and reaching a maximum of 40% restriction at 16 weeks and thereafter (as compared with food consumed by *ad libitum* fed controls) and this continued for 12 total weeks. Mice will be fed LabTreat™ Enrichment Tablets from Purina TestDiet® with either a control diet (5001) or a Food Restriction, Portion-Controlled Feeding regimen, and food intake will be monitored. This CR diet enhances health, extends lifespan in a variety of mouse genetic backgrounds (2), and has been previously characterized with regard to changes in metabolite levels during CR (1). Two mice will be housed in one cage with a divider to split the cage into two equal parts.

Oxygen consumption rate measurements

Oxygen consumption rate (OCR) was measured in differentiated shctr and shSirt3 C2C12 cells using the Seahorse XF24 Bioanalyzer. Briefly, 50,000 cells in DMEM were plated at 24 h before the experiment on Seahorse Biosciences 24-well culture plates and incubated at 37°C. OCR was measured before and after sequential addition of 2.5 μ M Oligomycin A, 10 μ M carbonylcyanide-p-trifluoromethoxy-phenylhydrazone (FCCP), and 2 μ M Antimycin A and Rotenone (final concentrations). Measurements were normalized to the number of cells/well at the end of the experiment.



SUPPLEMENTARY FIG. S7. No difference in the number of total mitochondria after genetic deletion or knockdown of *Sirt3*. (A) Total number of mitochondria in skeletal muscle was estimated by real-time quantitative PCR (qPCR) using the ratio of mitochondrial-encoded genes (NADH dehydrogenase 2, ATP synthase 6, and cytochrome oxidase subunit II) versus nuclear-encoded 18S rRNA after isolating DNA. Both *Sirt3* wild-type (WT) and knockout (KO) 12 month-old mice that had been used earlier for the treadmill experiments were used. (B) Same method as described in (A) was used to estimate total number of mitochondria in differentiated shctr C2C12 myotubes and sh*Sirt3* knockdown C2C12 myotubes.

Mitochondrial number

To estimate mitochondrial number, total DNA was extracted from skeletal muscle tissue or C2C12 cells using the QIAamp DNA mini kit. DNA was subject to qPCR using primers designed against mitochondrial-encoded genes NADH dehydrogenase 2, ATP synthase 6, and cytochrome oxidase subunit II versus nuclear-encoded 18S rRNA.

Exercise testing

For the endurance exercise protocol, 6- and 12 month-old *Sirt3*^{+/+} and *Sirt3*^{-/-} male mice were subjected to a resistance running test, using a variable speed belt treadmill that was enclosed in a plexiglass chamber with a stimulus device consisting of a shock grid attached to the rear of the belt. Mice were acclimated to the chamber for 3 consecutive days before the day of the running test by running for 5 min at 10 m/min. For the actual test, mice started running at 10 m/min at 0° incline. Maximum exercise capacity was determined by a graded increase in speed and/or incline to exhaustion, which was assumed when mice could not run on the treadmill despite the shocks. Mice were removed from the treadmill on exhaustion.

Cardiac function test

Cardiac magnetic resonance imaging (MRI) was performed at rest and during dobutamine stress. Mice were anesthetized with isoflurane, placed prone on a plastic cradle, head stabilized with a holder-bite bar and nosecone for isoflurane delivery, hydrated with subcutaneous 0.9% saline (~0.5–1 ml/25 g mouse), and monitored with a pressure transducer for respiration and rectal temperature probe. Conductive leads were placed for ECG acquisition. The mouse cradle and apparatus were placed in a volume MR coil with a warm air blower for body temperature control. A contrast agent (Gd-DTPA, Berlex) was delivered at 0.3 mmol/kg i.v. by tail vein cannulation. Short axis cine cardiac MRI scans were obtained: repetition time 9–10 ms,

echo time 3.4 ms, 4–5 averages, and 10 or more frames depending on heart rate. Cine scans were obtained on three slices at mid-ventricle, at baseline, and during dobutamine stress. Dobutamine was administered in two steps at 10 and 40 $\mu\text{g}/\text{kg}/\text{min}$ by a tail vein catheter. Ejection fractions were calculated for baseline and stress steps using CAAS_MRV_FARM software (Pie Medical Imaging).

High-fat “Western diet” (TD.88137; Harlan Teklad, Indianapolis, IN)

The TD.88137 is often referred to in the published scientific literature as the “Western” Diet (www.harlan.com/products_and_services/research_models_and_services/laboratory_animal_diets/teklad_custom_research_diets/atherogenic.hl). This is a purified diet with 21% anhydrous milkfat (butterfat), 34% sucrose, and a total of 0.2% cholesterol. The formula originated with researchers at Rockefeller University, and it is widely used with ApoE-deficient and other similar models. The diet used in this study contained (i) Total protein = 173 g/kg; (ii) Total fat = 212 g/kg (saturated 133 g/kg, monoun saturated 59 g/kg, and poly-saturated 9 g/kg), Total carbohydrates 485 g/kg, and sucrose 341 g/kg. The critical dietary features of this diet include Cholesterol (0.2% total cholesterol), total fat (21% by weight; 42% kcal from fat), high in saturated fatty acids (>60% of total fatty acids), and high sucrose (34% by weight). The mice used in this study were on this diet for 12 weeks.

Supplementary References

- Selman C, Kerrison ND, Cooray A, Piper MD, Lingard SJ, Barton RH, Schuster EF, Blanc E, Gems D, Nicholson JK, *et al.* Coordinated multitissue transcriptional and plasma metabolomic profiles following acute caloric restriction in mice. *Physiol Genomics* 27, 187–200, 2006.
- Turturro A, Witt WW, Lewis S, Hass BS, Lipman RD, and Hart RW. Growth curves and survival characteristics of the animals used in the Biomarkers of Aging Program. *J Gerontol* 54, B492–B501, 1999.

ATP Synthase alpha

<u>Species</u>	<u>K132 (125-137)</u>	<u>K161, K167 (158-170)</u>
Human	IKEGDIV K RTGAI	IDG K GPIG S KTRR
Mouse	IKEGDIV K RTGAI	IDG K GPIG S KTRR
Rat	IKEGDIV K RTGAI	IDG K GPVGS K IRR
Boar	IKEGDIV K RTGAI	IDG K GPIG S KTRR
Bovine	IKEGDIV K RTGAI	IDG K GPIG S KTRR
Orangutan	IKEGDIV K RTGAI	IDG K GPIG S KTRR
Chimpanzee	IKEGDIV K RTGAI	IDG K GPIG S KTRR
Atlantic Salmon	IKEGDIV K RTGAI	IDG K GPLG S SIRR
Zebrafish	IKEGDIV K RTGAI (K121)	IDG K GPLG S KERR (K160, K166)
C. elegans	IREGDIV K RTGAI (K117)	IDG K GPIANARRS (K146)

ATP Synthase alpha

<u>Species</u>	<u>K427, K434 (424-437)</u>	<u>K539 (533-545)</u>
Human	RAM K QVAGTM K LLEL	SEQSDAKL K EIVT
Mouse	RAM K QVAGTM K LLEL	SEQSDAKL K EIVT
Rat	RAM K QVAGTM K LLEL	SEQSDAKL K EIVT
Boar	RAM K QVAGTM K LLEL	SEQSDAKL K EIVT
Bovine	RAM K QVAGTM K LLEL	SEQSDAKL K EIVT
Orangutan	RAM K QVAGTM K LLEL	SEQSDAKL K EIVT
Chimpanzee	RAM K QVAGTM K LLEL	SEQSDAKL K EIVT
Atlantic Salmon	RAM K QVAGTM K LLEL	SETADAQL K QIVL
Zebrafish	RAM K QVAGTM K LLEL (K426, K433)	SEASDAKL K EIVL (K538)
C. elegans	KAM K QVAGSM K LLEL (K412, K419)	SPQTDAQLKDVVV

ATP Synthase beta

<u>Species</u>	<u>K197 (191-203)</u>	<u>K259 (253-265)</u>
Human	LLAPYA K GG K IGL	SGVINL K DATSKV
Mouse	LLAPYA K GG K IGL	SGVINL K DATSKV
Rat	LLAPYA K GG K IGL	SGVINL K DATSKV
Boar	LLAPYA K GG K IGL	SGVINL K DATSKV
Bovine	LLAPYA K GG K IGL (K198)	SGVINL K DATSKV
Orangutan	LLAPYA K GG K IGL (K310)	ILVLSTX K DATSKV (K372)
Chimpanzee	LLAPYA K GG K IGL S	GVINL K DATSKV
Atlantic Salmon	--	--
Zebrafish	LLAPYA K GG K IGL (K187)	SGVINL K DTTSKV (K248)
C. elegans	LLAPYA K GG K IGL (K206)	GGVIDL K GKNSKV (K268)

ATP Synthase gamma

<u>Species</u>	<u>K136, K138 (129-142)</u>	<u>K154 (148-160)</u>
Human	LVGIGD K IKGILY	QFLVAF K EVGRKP
Mouse	IVGVGE K IKGILY	QFLVSF K DVGRKP
Rat	IVGIG K IKSILY	QFLVSF K DVGRKP
Boar	-- --	
Bovine	IIGVGD K IRSILH	QFLVTF K EVGRRP
Orangutan	LVGIGD K IRGILY	QFLVAF K EVGRKP
Chimpanzee	LVGIGD K IRGILY	QFLVAF K EVGRKP
Atlantic Salmon	VVNVD K LRNILQ (K132)	YLLLSC K EVGRKP (150)
Zebrafish	VVNIGD K LRGLLY (K131)	HILLNC K EVGRKP
C. elegans	--	--

SUPPLEMENTARY FIG. S8. ATP synthase alpha, beta, and gamma contain evolutionarily conserved lysines. The synthase alpha, beta, and gamma proteins were BLASTed from multiple species to identify potentially conserved reversible acetyl-lysine residues that were also found to be altered in murine and human proteomic studies as shown in Tables 1–3. Conserved lysines are shown in red, and amino-acid sequence numbers are shown.